Bollettino di Geofisica Teorica ed Applicata Vol. 59, n. 2, pp. 179-192; June 2018
DOI 10.4430/bgta0229

Radiation from a vertical electric dipole above an inhomogeneous soil plane over the Earth

T. Mosayebidorcheh, F. Hosseinibalam and S. Hassanzadeh

Department of Physics, University of Isfahan, Iran

(Received: 9 December 2017; accepted: 22 March 2018)

ABSTRACT Despite the great work on the propagation of vertical electrical dipole (VED), the effect of inhomogeneous soil texture on VED electromagnetic radiation above the soil is not understood. Using Fourier integral transform, the equations of the magnetic fields for each region is obtained. Also, the electrical permittivity and conductivity variation of soil texture with humidity is extracted. Having humidity dependency of soil to depth, the electrical permittivity and conductivity of soil texture in each depth can be calculated. The maximum changes of the value of integration will be 0.1% by doubling the number of semi-intervals, so the magnetic field is validated. In the cases of clay or sand, the magnetic fields inside and above the Earth are the same at the frequency of 1 MHz. But the magnetic field differences for clay and sand inside the Earth at the frequency of 50 MHz are significant. In the distances far from vertical electrical dipole in the air, the magnetic fields are the same in different heights because the distances to the points come closer in different heights and high radial distances.

Key words: vertical electric dipole, electromagnetic radiation, integral Fourier transformation, soil texture.

1. Introduction

Electromagnetic wave propagation radiated by a horizontal electric dipole (HED) or a vertical electric dipole (VED), above or inside the ground has been studied for a while. There are two methods to investigate this. The first one is to solve Maxwell equations assuming that the Earth, atmospheric and dielectric layers are relatively flat. The other method accounts for the spherical shape of the Earth and the atmosphere, and the sum of spherical harmonics will be obtained (Mosayebidorcheh *et al.*, 2017). Tending the radius of the Earth to infinity in the second one, leads to the first method. In the case that the wavelengths are much smaller than the radius of the Earth, the spherical shape of the earth can be neglected.

The first analytical solution of the propagation of the electromagnetic waves along the planar boundary between the atmosphere and the Earth was performed by Zenneck (1907). That time, the existence and significance of the ionosphere were unknown. Many investigators, such as Wait (1953, 1956, 1957, 1970, 1990a, 1990b), King (1991), King *et al.* (1992), and King and Sandler (1994a, 1994b), have made the subsequent developments concerning the electromagnetic fields of a dipole source in the homogeneous multilayered regions. Using surface-impedance technique for two-layered or multilayered regions, extensive studies have

been conducted. In the 1990s, further developments were made by King (1991), King *et al.* (1992), and King and Sandler (1994a, 1994b). Later, Wait (1998) presented a comment on King and Sandler (1994a) article and contended that they had missed the terms of the trapped surface wave, as trapped surface wave varies in terms of $\rho^{-\frac{1}{2}}$ in the far region. Also, Collin (2004) found that King and Sandler (1994a, 1994b) overlooked the term of the trapped surface wave. In order to clarify the debates on the trapped surface wave, in the 2000s, many investigators reconsidered the problem (Zhang and Pan, 2002; Li and Lu, 2005; Zhang *et al.*, 2005). Li and Li (2017) used dipole source (including antenna azimuth, dip, and horizontal positions) and presented a joint inversion method for the transmitter navigation and the seafloor resistivity for frequency domain marine controlled-source electromagnetic (CSEM) data. Also they presented wavenumber domain (WD) electromagnetic field expressions at any depth in a layered conductivity Earth due to both the HEDS and VEDS (Li and Li, 2016). Key (2009) used numerical methods for 1D forward modelling and inversion of marine CSEM data to examine the inherent resolution of various acquisition configurations to thin resistive layers simulating offshore hydrocarbon reservoirs.

Samaddar (1967) formulated the problem of radiation from a VED in an inhomogeneous half-space. The detailed calculations are carried out for a suitable profile. They showed that in an inhomogeneous semi-infinite (or infinite) medium, the far field energy may be propagated also in the angular direction (θ-direction). In this research the effect of soil texture on the propagation of electromagnetic waves by a VED above the soil is investigated.

2. Basic theory

2.1. The model

The geometry of the problem (Fig. 1) is defined as an n+2 layers with n inhomogeneous layers (each layer thickness is l_j, j=1, 2,⋯, n) between air as upper layer ($z>0$) and the Earth as lower layer ($z<-l$). An ideal VED is located at point (0, 0, d). The electrical conductivity and permittivity of the air are zero and ε_0, respectively. Also, the electrical conductivity and permittivity of the Earth are σ_g and ε_g, respectively. The electrical conductivity and permittivity of the each dielectric layers are the function of z and they are represented by $\sigma_j(z)$ and $\varepsilon_j(z)$, respectively.

2.2. Integral Fourier transformation and Maxwell equations

If time dependency of electromagnetic fields is as e^{-iwt}, the Maxwell equations are as follows:

$$\nabla \times \mathbf{E}_j = i\omega \mathbf{B}_j , \tag{1}$$

$$\nabla \times \mathbf{B}_j = -\frac{ik_j^2}{\omega}\mathbf{E}_j + \mu_0 \mathbf{J} , \tag{2}$$

where

$$\mathbf{J} = \hat{\mathbf{z}}\delta(x)\delta(y)\delta(z-d), \tag{3}$$

$$k = \sqrt{\mu_0 \varepsilon_j \omega^2 + i\mu_0 \sigma_j \omega}; \quad j = 0, 1, 2, 3, \ , n, g \tag{4}$$

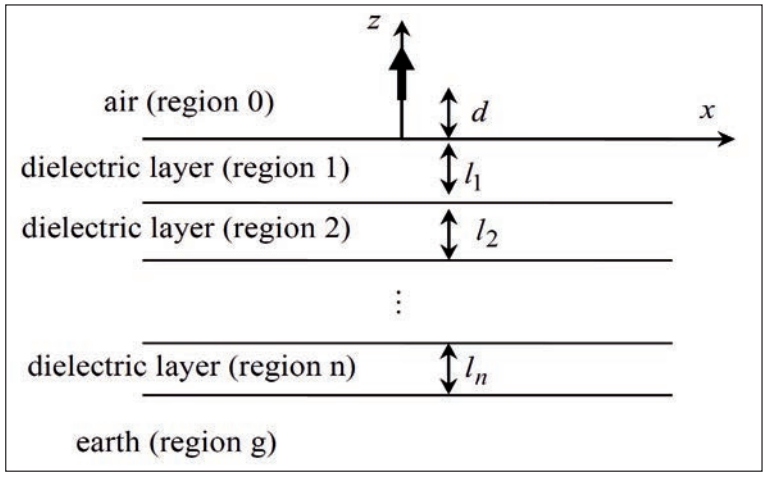

Fig. 1 - Geometry of the problem.

where ω, $\varepsilon_j=\varepsilon_{rj}\varepsilon_0, \sigma_j, \mu_0$, and k_j are angular frequency, electrical permittivity of the jth medium, electrical conductivity of the jth medium, the magnetic permeability of the vacuum, and the wave number of the jth medium, respectively.

To obtain the explicit relationships for the components of the field, Fourier transforms are used.

$$\mathbf{E}_j(x,y,z)=\frac{1}{(2\pi)^2}\int_{-\infty}^{\infty}d\xi\int_{-\infty}^{\infty}d\eta\, e^{-i(\xi x+\eta y)}\overline{\mathbf{E}}_j(\xi,\eta,z), \tag{5}$$

$$\mathbf{B}_j(x,y,z)=\frac{1}{(2\pi)^2}\int_{-\infty}^{\infty}d\xi\int_{-\infty}^{\infty}d\eta\, e^{-i(\xi x+\eta y)}\overline{\mathbf{B}}_j(\xi,\eta,z), \tag{6}$$

$$\mathbf{J}_j(x,y,z)=\frac{1}{(2\pi)^2}\int_{-\infty}^{\infty}d\xi\int_{-\infty}^{\infty}d\eta\, e^{-i(\xi x+\eta y)}\overline{\mathbf{J}}_j(\xi,\eta,z), \tag{7}$$

where

$$\overline{\mathbf{J}}(\xi,\eta,z)=\delta(z-d)\hat{\mathbf{z}}, \tag{8}$$

Noting that with rotational symmetry, $B_z = 0$. Regarding the Maxwell equations, the following result is obtained:

$$-i\eta\overline{E}_{jz}-\frac{\partial\overline{E}_{jy}}{\partial z}=i\omega\overline{B}_{jx},\quad \frac{\partial\overline{E}_{jx}}{\partial z}+i\xi\overline{E}_{jz}=i\omega\overline{B}_{jy},\quad -i\xi\overline{E}_{jy}+i\eta\overline{E}_{jx}=0,$$

$$\frac{\partial\overline{B}_{jy}}{\partial z}=\frac{ik_j^2}{\omega}\overline{E}_{jx},\quad \frac{\partial\overline{B}_{jx}}{\partial z}=-\frac{ik_j^2}{\omega}\overline{E}_{jy},$$

$$-i\xi\overline{B}_{jy}+i\eta\overline{B}_{jx}=-\frac{ik_j^2}{\omega}\overline{E}_{jz}+\mu_0\delta(z-d),\quad j=0,1,2,\quad ,n,g, \tag{9}$$

where

$$\gamma_j=\left(k_j^2-\xi^2-\eta^2\right)^{\frac{1}{2}},\quad j=0,1,2,\ ,n,\ g \tag{10}$$

The equations for the air, for the inhomogeneous dielectric layers, and for the Earth are as follows:

$$\frac{\partial^2 \overline{B}_{0x}}{\partial z^2} + \gamma_0^2 \overline{B}_{0x} = \frac{i\eta\mu_0}{2\pi}\delta(z-d), \tag{11}$$

$$\frac{\partial^2 \overline{B}_{jx}}{\partial z^2} - \frac{2}{k_j}\frac{\partial k_j}{\partial z}\frac{\partial \overline{B}_{jx}}{\partial z} + \gamma_j^2 \overline{B}_{jx} = 0, \quad j = 1, 2, \quad , n \tag{12}$$

$$\frac{\partial^2 \overline{B}_{gx}}{\partial z^2} + \gamma_g^2 \overline{B}_{gx} = 0, \tag{13}$$

The solutions to these equations may be obtained as below:

$$\overline{B}_{0x} = \eta C_0 e^{i\gamma_0 z} - \frac{\eta\mu_0}{2\gamma_0} e^{i\gamma_0|z-d|}, \tag{14}$$

$$\overline{B}_{jx} = \eta C_j f_j(z,\lambda) + \eta D_j g_j(z,\lambda), \quad j = 1, 2, \quad , n, \tag{15}$$

$$\overline{B}_{gx} = \eta C_g e^{-i\gamma_g z}, \tag{16}$$

where $f_j(z,\lambda)$ and $g_j(z,\lambda)$ are two solutions of differential equation for each inhomogeneous dielectric layer, where these are linear independent functions. In order that $f_j(z,\lambda)$ and $g_j(z,\lambda)$ be linearly independent, we assume that $f_j(Z_j,\lambda)=1$ and $\frac{df_j}{dz}(Z_j,\lambda)=0$, and also $g_j(Z_j,\lambda)=0$ and $\frac{dg_j}{dz}(Z_j,\lambda)=1$. Since Wronskian of these two functions at the point of $z_j=Z_j$ is not zero, these two functions are linearly independent. In this problem, the boundary conditions are as follows:

$$\overline{B}_{0x}(\xi,\eta,0) = \overline{B}_{1x}(\xi,\eta,0), \tag{17}$$

$$\overline{B}_{jx}(\xi,\eta,Z_j) = \overline{B}_{j+1,x}(\xi,\eta,Z_j), \quad j = 1, 2, \quad , n-1, \tag{18}$$

$$\overline{B}_{nx}(\xi,\eta,Z_n) = \overline{B}_{gx}(\xi,\eta,Z_n), \tag{19}$$

$$\frac{\partial \overline{B}_{0x}(0)}{\partial z} = \frac{\partial \overline{B}_{1x}(0)}{\partial z}, \tag{20}$$

$$\frac{\partial \overline{B}_{jx}(Z_j)}{\partial z} = \frac{\partial \overline{B}_{j+1,x}(Z_j)}{\partial z}, \tag{21}$$

$$\frac{\partial \overline{B}_{nx}(Z_j)}{\partial z} = \frac{\partial \overline{B}_{n+1,x}(Z_j)}{\partial z}, \tag{22}$$

where

$$Z_j = \begin{cases} 0 & j = 0 \\ \sum_{p=1}^{j} l_p, & j = 1, 2, \quad , n \end{cases} \tag{23}$$

With regard to selected boundary conditions for the functions $f_j(z,\lambda)$ and $g_j(z,\lambda)$, the boundary conditions of the problem are as follows:

$$\eta C_0 - \frac{\eta\mu_0}{2\gamma_0} e^{i\gamma_0 d} = \eta C_1 , \tag{24}$$

$$\eta C_j f_j\left(Z_j,\lambda\right) + \eta D_j g_j\left(Z_j,\lambda\right) = \eta C_{j+1} , \quad j = 1, 2, \quad , n-1, \tag{25}$$

$$\eta C_n f_n\left(Z_n,\lambda\right) + \eta D_n g_n\left(Z_n,\lambda\right) = \eta C_g e^{-i\gamma_g Z_n} , \tag{26}$$

$$i\eta\gamma_0 C_0 + \frac{i\eta\mu_0}{2} e^{i\gamma_0 d} = \eta D_1 , \tag{27}$$

$$\eta C_j \frac{df_j}{dz}\left(Z_j,\lambda\right) + \eta D_j \frac{dg_j}{dz}\left(Z_j,\lambda\right) = \eta D_{j+1} , \quad j = 1, 2, \quad , n-1, \tag{28}$$

$$\eta C_n \frac{df_n}{dz}\left(Z_n,\lambda\right) + \eta D_n \frac{dg_n}{dz}\left(Z_n,\lambda\right) = -i\gamma_g \eta C_g e^{-i\gamma_g Z_n} , \tag{29}$$

The unknown coefficients are obtained using Eqs. 24 to 29.

2.3. Solving differential equation for inhomogeneous medium

Finite difference method is used to solve differential equation of inhomogeneous medium. In this case, the first and second derivations of magnetic field are as follows:

$$\frac{\partial \overline{B}_{jx}}{\partial z} = \frac{\overline{B}_{jx}(m+1) - \overline{B}_{jx}(m)}{\Delta z}, \tag{30}$$

$$\frac{\partial^2 \overline{B}_{jx}}{\partial z^2} = \frac{\overline{B}_{jx}(m+1) - 2\overline{B}_{jx}(m) + \overline{B}_{jx}(m-1)}{\Delta z^2}, \tag{31}$$

And finally, the magnetic field of each layer is:

$$\overline{B}_{jx}(m+1) = \frac{1}{\left(\frac{2}{k_j}\frac{\partial k_j}{\partial z}\right)\Big|_{z=z_m} \Delta z - 1} \left[-2\overline{B}_{jx}(m) + \overline{B}_{jx}(m-1) + \left(\frac{2}{k_j}\frac{\partial k_j}{\partial z}\right)\Big|_{z=z_m} \overline{B}_{jx}(m)\Delta z + \gamma_j^2 \overline{B}_{jx}(m)\Delta z^2 \right], \tag{32}$$

where $z_m = m\Delta z$, and the functions $f_j(z,\lambda)$ and $g_j(z,\lambda)$ are obtained in each point. To determine magnetic field in inhomogeneous region, it is necessary to calculate that regional wave number and its dependence to the depth of soil. The relationship between wave number and depth is discussed in the next section.

2.4. Permittivity and electrical conductivity variations of soil with depth

The electrical permittivity and conductivity of soil are depended on texture and moisture of the soil, and moisture of the soil changes with depth. By solving Richard's equation, the relation of the soil moisture changes with depth can be obtained. Richard's equation for one-dimensional water flow in soil is as below (Ross, 1990):

$$\frac{\partial \vartheta}{\partial t} = \frac{\partial}{\partial z}\left[K\left(d\frac{\partial p}{\partial z} - S \right) \right], \tag{33}$$

where

$\vartheta(\psi,z)$ = volumetric water content;

t = time;

z = space coordinate in direction of flow;

$K(\vartheta,z)$ = hydraulic conductivity;

$\psi(p)$ = matric potential;

$d = d(p) = \dfrac{d\psi}{dp}$;

$S = -\dfrac{dZ}{dz}$ where Z is elevation.

This equation is solved for different textures of soil. The dependence of soil moisture changes with depth, for clay and sand, are shown by Fig. 2. The best curve is plotted for each panel. The best equations of soil for these two textures are:

$$\vartheta = 0.183\tanh\left(0.2315z + 3.061\right) + 0.3047, \quad \text{for clay } (z \text{ in cm}), \tag{34}$$

$$\vartheta = 0.1292\tanh\left(2.22z + 44.43\right) + 1.313e^{0.001857z} - 1.146, \quad \text{for sand } (z \text{ in cm}), \tag{35}$$

The goodness of fit is evaluated through the adjusted R-squared and the Root Mean Squared Error (RMSE). The adjusted R-squared and RMSE are 0.998 and 0.005413 for clay, and 0.9809 and 0.0138 for sand respectively.

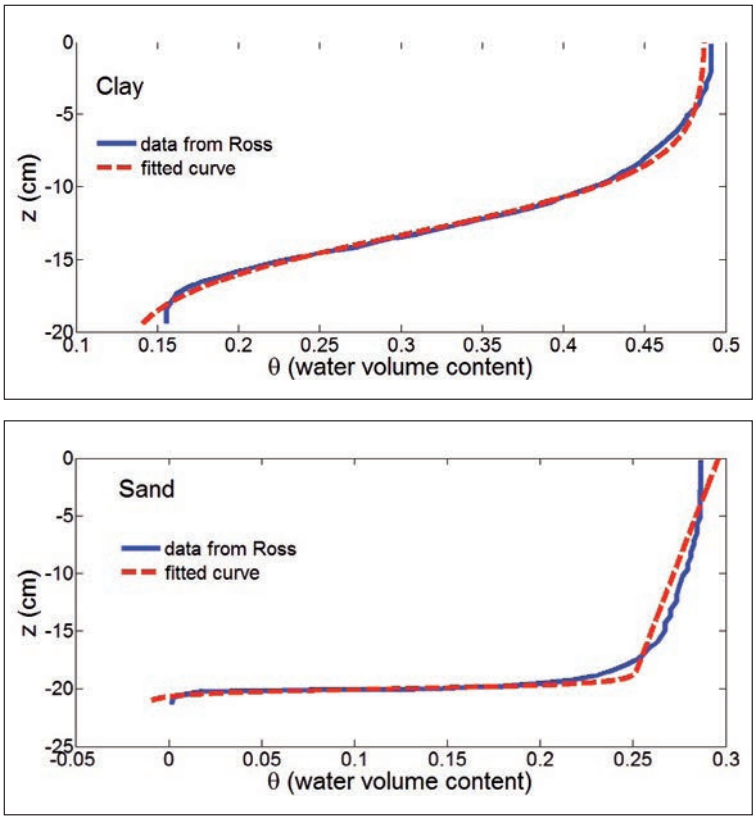

a

b

Fig. 2 - Soil moisture variation diagram in terms of depth and the best crossing curve: a) clay; b) sand.

The moisture of the soil is fixed in depth of 18.35 and 20.77 cm from the air-soil interface for clay and sand, respectively. So below these depths, considering the stability of soil electric characteristics, the Earth can be considered as third layer. Due to soil moisture variations, the electrical permittivity and conductivity of soil change. Fig. 3 shows the electrical permittivity variations of clay and sand with moisture, at frequency of 1 MHz, respectively (Campbell, 1990). In addition, the best curve crossing of each diagrams are plotted. The equations are as follow:

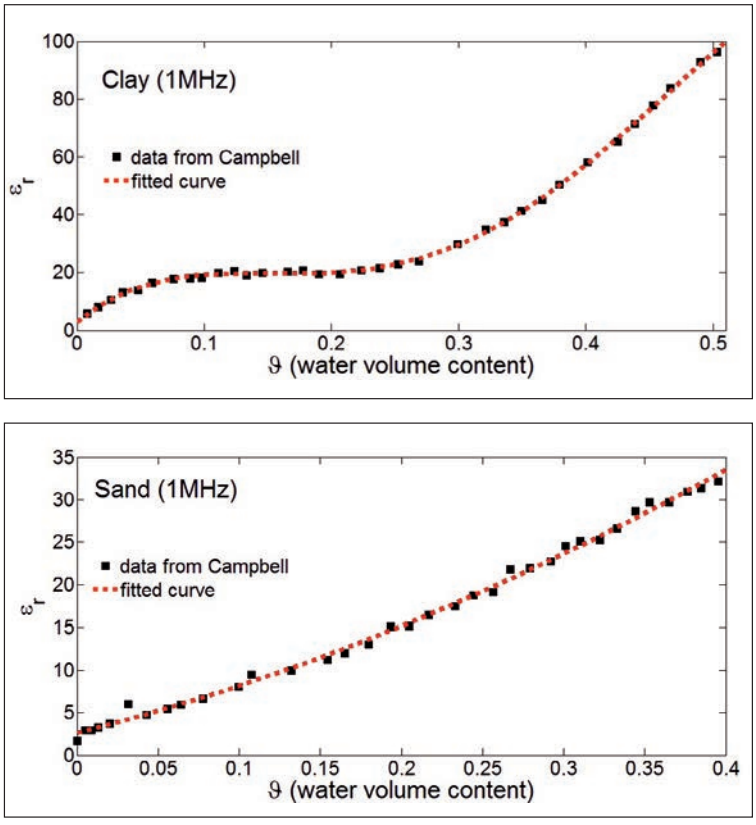

Fig. 3 - Electric permittivity variations diagram at the frequency of 1 MHz in terms of the moisture and the best crossing curve: a) clay; b) sand.

$$\varepsilon_r = -6450\vartheta^4 + 7935\vartheta^3 - 2703\vartheta^2 + 360.4\vartheta + 2.81, \quad \text{for clay}, \tag{36}$$

$$\varepsilon_r = 72.22\vartheta^2 + 48.39\vartheta + 2.611, \quad \text{for sand}. \tag{37}$$

The adjusted R-squared and RMSE are 0.9993 and 0.6673 for clay, and 0.9961 and 0.6137 for sand respectively.

The loss tangent data measured by Campbell (1990) is required to calculate electrical conductivity. Fig. 4 indicates the loss tangent diagram for clay at the 1 MHz frequency in terms of moisture. The best curve equation crossing the data is as follows:

$$\tan\delta = -5.832\tanh\left(-7.076\,\vartheta + 1.65\right) + 5.872\,. \tag{38}$$

The adjusted R-squared and RMSE are 0.9925 and 0.3622 for clay respectively. Also, the following relation between loss tangent and conductivity is in the form of:

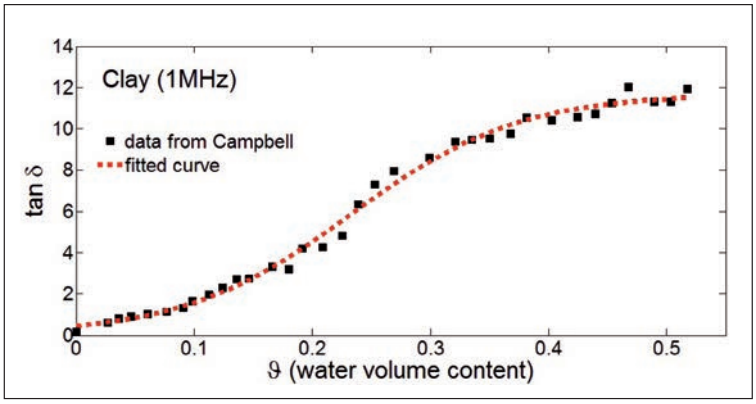

Fig. 4 - Loss tangent variation diagram for clay at the frequency of 1 MHz in terms of moisture, and the best curve crossing it.

$$\tan\delta = \frac{\sigma}{\omega\varepsilon_r\varepsilon_0}\,. \tag{39}$$

The magnetic field can be determined by the relationship between electrical permittivity and conductivity with depth. In the next section the magnetic fields in any region will be formulated.

3. Results and discussions

Considering Eqs. 34 to 39, the electrical permittivity, conductivity and the wave number of soil can be obtained in terms of depth from the soil-air interface. In the next step, the functions of $f_j(z,\lambda)$ and $g_j(z,\lambda)$ in the soil are derived and the unknown coefficients are verified by boundary conditions. Using reverse Fourier integral transformation of magnetic field in each region, the following equations are obtained:

$$B_{0\varphi} = \frac{-i}{2\pi}\int_0^\infty J_1(\lambda\rho)\left(C_0 e^{i\gamma_0 z} - \frac{\mu_0}{2\gamma_0}e^{i\gamma_0|z-d|}\right)\lambda^2 d\lambda\,, \tag{40}$$

$$B_{1\varphi} = \frac{-i}{2\pi}\int_0^\infty J_1(\lambda\rho)\left(C_1 f_1(z,\lambda) + D_1 g_1(z,\lambda)\right)\lambda^2 d\lambda\,, \tag{41}$$

$$B_{g\varphi} = \frac{-i}{2\pi}\int_0^\infty J_1(\lambda\rho) C_g e^{-i\gamma_g z}\lambda^2 d\lambda\,, \tag{42}$$

To integrate from these equations, the change of variables $\lambda = -1 + \frac{1}{t}$ is used, with an interval of integration between zero and one. Using Simpson method and dividing the interval of integration to parts, numerical integration is calculated. By doubling the number of N, the maximum changes of the value of integration will be 0.1%, therefore, the obtained results are validated.

In this problem, two-layered approximation can be utilized. In this case, different parts affect the magnetic fields: the direct field of VED, the reflected field due to an ideal image of VED, and the surface-wave terms. The summation of these terms are as follow (King *et al.*, 1992):

$$B_{0\varphi}^{app}(\rho,z)=\frac{-\mu_0}{2\pi}\left[\frac{e^{ik_0r_1}}{2}\left(\frac{\rho}{r_1}\right)\left(\frac{ik_0}{r_1}-\frac{1}{r_1^2}\right)+\frac{e^{ik_0r_2}}{2}\left(\frac{\rho}{r_2}\right)\left(\frac{ik_0}{r_2}-\frac{1}{r_2^2}\right)\right.$$
$$\left.-e^{ik_0r_2}\,\frac{k_0^3}{k_1}\left(\frac{\pi}{k_1r_2}\right)^{\frac{1}{2}}e^{-iP_2}F(P)\right], \qquad (43)$$

where

$$r_1=\sqrt{\rho^2+(z-d)^2}\,,r_1=\sqrt{\rho^2+(z+d)^2}\,,S_2=\frac{k_0^3r_2}{2k_1^2},R=\frac{k_0^3\rho}{2k_1^2},Z'=\frac{k_0^2z}{2k_1},D=\frac{k_0^2d}{2k_1},$$
$$P_2=S_2\left(\frac{S_2+Z'+D}{R}\right)^2,F(P_2)=\int_{P_2}^{\infty}\frac{e^{it}}{\sqrt{2\pi t}}dt\ . \qquad (44)$$

So, in the first approximation, the soil inhomogeneity effect can be overlooked. In this case, the results show that for clay and sand in the depth of 18.35 and 20.77 cm from air-soil interface, respectively, the moisture is fixed. Due to fixing the moisture, the whole Earth and soil are considered as a layer with the same permittivity and electrical conductivity. To show the effect of inhomogeneity of soil layer, the approximated and exact solutions are compared.

The magnetic field is investigated here due to its different applications in geophysics, such as ground magnetic method, airborne magnetic method, geomagnetic depth sounding (GDS), magnetovariational sounding (MVS), magnetotelluric sounding (MS), audiofrequency magnetotellurics (AMT), audiofrequency magnetic method (AFMAG), magnetic induced polarisation (MIP), magnetometric resistivity method (MMR), very low frequency (VLF), and in palaeomagnetism (Roy, 2007). Fig. 5 shows the magnetic field in two cases in which soil is clay or sand at the frequency of 1 MHz. Approximate and exact magnetic fields are plotted for each height (z = 1, 2, 5 m). As evidenced by the figures, the exact magnetic fields in the case of clay or sand, in different heights, are the same. This is due to the fact that the wavelength is much bigger than inhomogeneous layer thickness at the frequency of 1 MHz, and the effect of electrical conductivity in the reflected wave is not much significant. In the distances far from VED, the magnetic fields are the same in different heights, because in high ρ values the point distances of VED in different heights come close. In addition, approximate and exact magnetic fields in short distances from the VED are relatively the same, since in short distances, the effect of direct field and the reflected field due to an ideal image of VED is dominated. Distancing from dipole, the approximate and exact fields difference would be bigger due to the effect of inhomogeneous soil layer.

The Fig. 6 shows the magnetic field in two cases in which the soil is clay or sand at the frequency of 50 MHz. The approximate and exact magnetic fields for each height are plotted (z = 1, 2 m). Due to rising the frequency, the soil and Earth electrical conductivity increase sand consequently the wave reflection effect arises. As the result the magnetic field becomes greater. There is not much difference between the approximate and exact fields in short distances from VED, similar to Fig. 5.

Figs. 7 and 8 show the magnetic fields inside the Earth in the frequencies of 1 and 50 MHz in different depths. At the frequency of 1 MHz, the slight difference between the magnetic fields in cases of clay and sand is due to small weakening of waves. But the mentioned difference is significant at the frequency of 50 MHz, which is due to the high frequency and the electrical conductivity difference between sand and clay.

4. Conclusion

The main objective of this research is to investigate the effect of soil texture on the propagation of electromagnetic waves by a VED above the soil. For this purpose, using Fourier integral transform, the equations of the magnetic fields for each region is obtained. Also, the electrical permittivity and conductivity variation of soil texture with humidity is extracted. Having humidity dependency of soil to depth, the electrical permittivity and conductivity of soil texture in each depth can be calculated. The unknown coefficients are obtained using the boundary conditions. The integral form of the magnetic fields is obtained. Using change of variables, the interval of integration is changed from zero to one rather than zero to infinity. The maximum changes of the value of integration will be 0.1% by doubling the number of , so the magnetic field is validated. In this article, two textures of soil, sand and clay, are investigated and the results are as below:

- in the cases of clay or sand, the exact magnetic fields in different heights are the same, since the effect of electrical conductivity in the reflected wave is not much significant at 1 MHz frequency;

- in the distances far from the VED, the magnetic fields are the same in different heights because the distances to the points come closer in different heights and high values;

- in short distances, the effect of direct field and reflected field due to an ideal image is dominated. Therefore, the approximate and exact magnetic fields are relatively the same;

- distancing from the dipole, the difference between the approximate and exact fields are significant due to the effect of soil layer;

- the magnetic fields inside the Earth for clay and sand in different depths, and at the frequency of 1 MHz are the same;

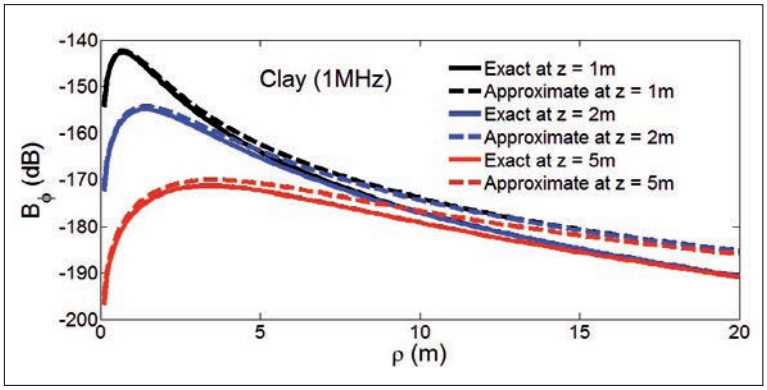

Fig. 5 - Magnetic field $B_{0\varphi}$ in the air at the frequency of 1 MHz in terms of radial distances from the VED: a) soil is clay; b) soil is sand. The approximate fields for each height are plotted ($d = 0$).

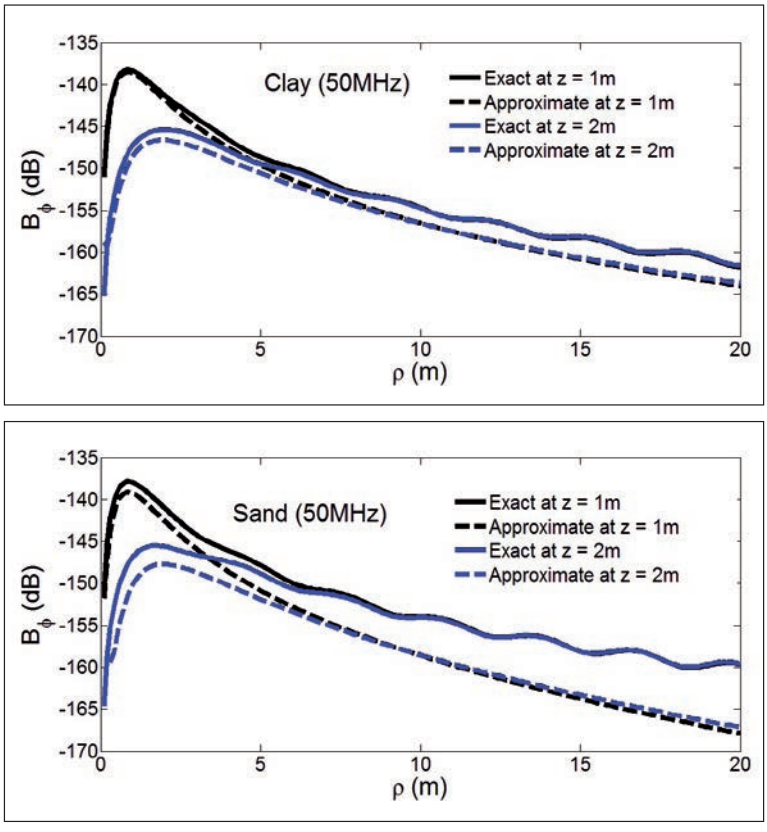

Fig. 6 - Magnetic field $B_{0\varphi}$ in the air at the frequency of 50 MHz in terms of radial distances from the VED: a) soil is clay; b) soil is sand. The approximate fields for each height are plotted ($d = 0$).

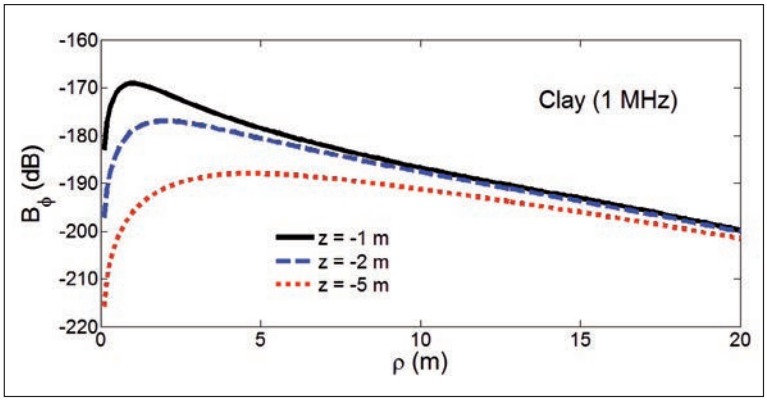

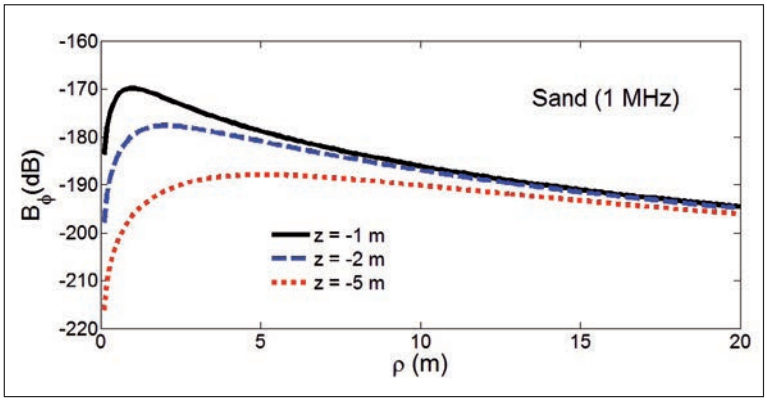

Fig. 7 - Magnetic field in the Earth in different depths at the frequency of 1 MHz in terms of radial distances from the VED: a) soil is clay; b) soil is sand ($d = 0$).

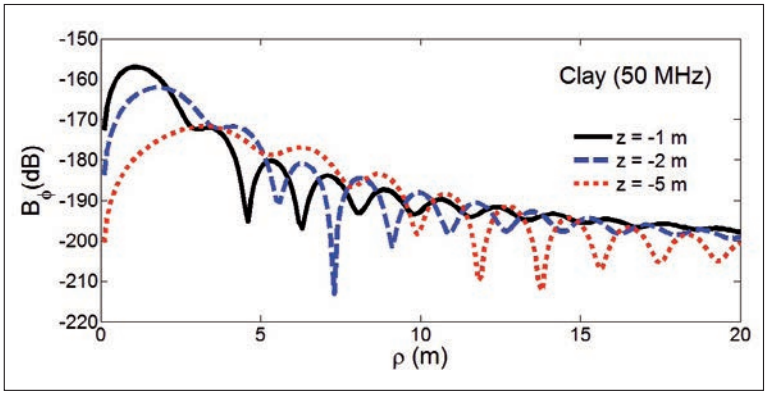

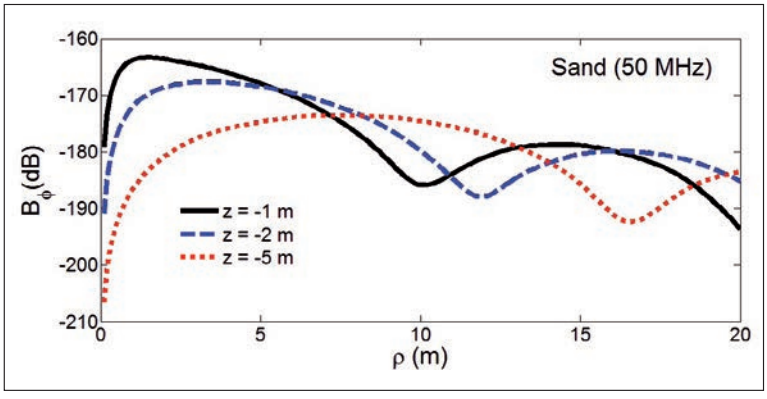

Fig. 8 - Magnetic field in the Earth in different depths at the frequency of 50 MHz in terms of radial distances from the VED: a) soil is clay; b) soil is sand ($d = 0$).

- the magnetic field differences inside the Earth for clay and sand at the frequency of 50 MHz are significant, which is due to the high frequency and the electrical conductivity difference between sand and clay.

References

Campbell J.E.; 1990: *Dielectric properties and influence of conductivity in soils at one to fifty megahertz*. Soil Sci. Soc. Am. J., **54,** 332-341.

Collin R.E.; 2004: *Hertzian dipole radiating over a lossy earth or sea: some early and late 20th-century controversies*. IEEE Antennas Propag. Mag., **46,** 64-79.

Key K.; 2009: *1D inversion of multicomponent, multifrequency marine CSEM data: methodology and synthetic studies for resolving thin resistive layers*. Geophys., **74,** F9-F20.

King R.W.P.; 1991: *The electromagnetic field of a horizontal electric dipole in the presence of a three-layered region*. J. Appl. Phys., **69,** 7987-7995.

King R.W.P. and Sandler S.S.; 1994a: *The electromagnetic field of a vertical electric dipole in the presence of a three-layered region*. Radio Sci., **29,** 97-113.

King R.W.P. and Sandler S.S.; 1994b: *The electromagnetic field of a vertical electric dipole over the earth or sea*. IEEE Trans. Antennas Propag., **42,** 382-389.

King R.W.P., Owens M. and Wu T.T.; 1992: *Lateral electromagnetic waves: theory and applications to communications, geophysical exploration, and remote sensing*. Springer-Verlag, Berlin Heidelberg, Germany, 774 pp.

Li G. and Li Y.; 2017: *Joint inversion for transmitter navigation and seafloor resistivity for frequency-domain marine CSEM data*. J. Appl. Geophys., **136**, 178-189.

Li Y. and Li G.; 2016: *Electromagnetic field expressions in the wavenumber domain from both the horizontal and vertical electric dipoles*. J. Geophys. Eng., **13,** 505-515.

Li K. and Lu Y.; 2005: *Electromagnetic field generated by a horizontal electric dipole near the surface of a planar perfect conductor coated with a uniaxial layer*. IEEE Trans. Antennas Propag., **53,** 3191-3200.

Mosayebidorcheh T., Hosseinibalam F. and Hassanzadeh S.; 2017: *Analytical solution of electromagnetic radiation by a vertical electric dipole inside the earth and the effect of atmospheric electrical conductivity inhomogeneity*. Adv. Space Res., **60**, 1949-1957, doi: org/10.1016/j.asr.2017.07.34.

Ross P.J.; 1990: *Efficient numerical methods for infiltration using Richards' equation*. Water Resour. Res., **26,** 279-290.

Roy K.K.; 2007: *Potential theory in applied geophysics*. Springer-Verlag Berlin Heidelberg, Germany, 650 pp.

Samaddar S.N.; 1967: *Radiation from a vertical electric dipole in an inhomogeneous half-space*. Proc. IEEE, **55,** 2023-2024.

Wait J.R.; 1953: *Radiation from a vertical electric dipole over a stratified ground*. IRE Trans. Antennas Propag., **1,** 9-12.

Wait J.R.; 1956: *Radiation from a vertical antenna over a curved stratified ground*. J. Res. Nat. Bur. Stand., **56,** 237-244.

Wait J.R.; 1957: *Excitation of surface waves on conducting, stratified, dielectric-clad, and corrugated surfaces*. J. Res. Nat. Bur. Stand., **59,** 365-377.

Wait J.R.; 1970: *Electromagnetic waves in stratified media (2nd ed.)*. Pergamon Press, New York, NY, USA, 620 pp.

Wait J.R.; 1990a: *Electromagnetic fields of a vertical electric dipole over a laterally anisotropic surface.* IEEE Trans. Antennas Propag., **38,** 1719-1723.

Wait J.R.; 1990b: *Radiation from vertical electric dipole located over laterally anisotropic groundplane*. Electron. Lett., **26,** 74-76.

Wait J.R.; 1998: *Comment on "The electromagnetic field of a vertical electric dipole in the presence of a three-layered region" by Ronold W.P. King and Sheldon S. Sandler*. Radio Sci., **33,** 251-253.

Zenneck J.; 1907: *Über die Fortpflanzung ebener elektromagnetischer Wellen längs einer ebenen Leiterfläche und ihre Beziehung zur drahtlosen Telegraphie*. Ann. Phys., **328,** 846-866.

Zhang H.-Q. and Pan W.-Y.; 2002: *Electromagnetic field of a vertical electric dipole on a perfect conductor coated with a dielectric layer*. Radio Sci., **37**, 13-1-13-7.

Zhang H.-Q., Pan W.-Y., Li K. and Shen K.-X.; 2005: *Electromagnetic field for a horizontal electric dipole buried inside a dielectric layer coated high lossy half space*. Progr. Electromagn. Res., **50,** 163-186.

Corresponding author: Fahimeh Hosseinibalam
Department of Physics, University of Isfahan
Isfahan 81746-73441, Iran
Phone: +98 31793 4823; e-mail: fhb@sci.ui.ac.ir